INVESTIGATION OF THE INRUSH PHENOMENON
A QUASI-STATIONARY APPROACH IN THE HARMONIC DOMAIN

Nikola Rajaković* **Adam Semlyen**

Department of Electrical Engineering
University of Toronto
Toronto, Ontario, Canada

*On leave from University of Belgrade, Belgrade, Yugoslavia

Abstract - At the energization of transformers strong saturation and very high (inrush) currents may result which often last tens of seconds or even a few minutes. Because of the slow attenuation, the inrush phenomenon may be examined by phasor representations in the harmonic domain, i.e. as a quasi steady state phenomenon. In this paper harmonic domain analysis is used, including the d.c. component and even harmonics, to obtain a sequence of steady state "images" which constitute the complete picture of the inrush phenomenon. This methodology is similar to the traditional transient stability analysis of machines with mechanical oscillations. The advantage of the method is its robustness, compared to a time domain simulation with sufficiently small time steps to accurately represent the wave shapes of currents and voltages over a relatively long time span.

The calculations and results are given for single and three-phase transformers of different configurations.

Keywords: Inrush Current, Energization, Transformers, Harmonics, Laminations, Saturation, Iron Core.

INTRODUCTION

Inrush currents are large currents observed at the energization of transformers and saturating reactors [1]. They often exceed in magnitude the normal operating currents and may last tens of seconds and even several minutes. Inrush currents have to be taken into account in the design of the protective relaying system but may have other significance as well, as for instance in problems of resonance or ferroresonance and generation of temporary overvoltages [2]. Reference [3] gives useful practical data related to the magnitude and time variation of inrush currents.

The inrush phenomenon is related to the saturating magnetization characteristic of the iron core and is well understood. However, because of its nonlinear nature, it can not be described accurately in closed form and can be reproduced only by tests or computer simulation. Reduced scale testing may however not reflect accurately the attenuation observed with full size devices, while numerical simulation in time domain is prone to accumulation of errors especially in the case of slowly attenuating inrush currents.

This paper presents an alternate method for the simulation of the inrush phenomenon. The fact of slow attenuation which makes time domain simulation difficult is exploited here by considering the phenomenon as quasi steady state. The approach is analogous to the method used in the study of transient stability where phasors are still used despite the fact that they are not constant. The slower dynamics of the system gives then a sequence of steady states which are the simulation steps of a complete transient (see Fig.9). In our case harmonic domain phasor analysis is used for the steady state analysis, as described in references [4] and [5] which, however, deal with balanced magnetization conditions. In order to apply these concepts to the analysis of the inrush phenomenon, unsymmetrical magnetization has been included by considering also even harmonics and, in particular, a d.c. component to reflect the attenuating bias flux. A sequence of steady states is calculated for a decreasing set of d.c. premagnetizing flux inputs. The solution of the remaining problem, the calculation of the time elapsed between steady state solutions, corresponds to the slow dynamics of the system, related to the attenuation of the d.c. component of the magnetizing current.

In references [4] and [5] periodic steady state phenomena are investigated directly in the harmonic domain by using the fact that convolutions in the harmonic (i.e. frequency) domain correspond to multiplications in the time domain. This permits the correct representation of nonlinear (magnetization) characteristics in the harmonic domain, provided that they are mathematically represented by polynomials. The method has been applied to examine the phenomena inside of saturating laminations by discretizing them into layers, which we have called sublaminations. Clearly, the option of discretizing the laminations exists for the study of inrush currents as well or, alternatively, one may consider a uniform flux distribution inside the laminations, for a simpler procedure. We have applied both methods in order to examine the limitations on accuracy incurred by the simpler approach. The latter is of course much less demanding on computational resources and is therefore the only reasonable choice for the modeling of the inrush phenomenon in three-phase transformers. We have found that for the inrush phenomenon the discretization of the laminations produces only negligible differences. This is a very important result but, since it is a negative one, we have relegated the presentation of the details of this computational procedure to Appendix 1.

COMPUTATIONAL PROCEDURE

The approach adopted in this paper for the calculation of inrush currents consists in discretizing the phenomenon over time in steps Δt, small enough to have a quasi-static condition over the duration of the time step. The latter is calculated by harmonic domain techniques, and yields a sequence of steady state images valid for discrete values of time. The time step Δt is variable and is calculated in a second stage for any two sequential steady state images. Thus the time step calculation determines the rate of attenuation of the inrush phenomenon.

The complexity of the calculations may increase significantly when three-phase transformers are considered. Therefore the single and the three-phase case are examined separately.

Single-Phase Transformer

D.C. Premagnetization

D.c. premagnetization is strictly speaking the effect of a remanence flux. However, the energization of a winding at a moment different from the voltage peak also results in an offset flux which is fully equivalent to the flux offset due to remanence. This can be seen from the following equation:

$$\Phi-\Phi_{rem}=\frac{1}{N}\int_0^t v\,dt=\frac{1}{N}\int_0^t V_{max}\cos(\omega t-\phi)dt=\frac{V_{max}\sin\phi}{N\omega}+\frac{V_{max}}{N\omega}\sin(\omega t-\phi) \quad (1)$$

89 WM 082-9 PWRD A paper recommended and approved by the IEEE Transformers Committee of the IEEE Power Engineering Society for presentation at the IEEE/PES 1989 Winter Meeting, New York, New York, January 29 - Febreuary 3, 1989. Manuscript submitted July 14, 1988; made available for printing November 14, 1988.

where ϕ is the angle of the off-peak switching and the first term at the right side represents the resultant d.c. flux offset. Correspondingly, we will consider as d.c. premagnetization the combined effect of remanence and off-peak switching. It is of fundamental significance in the inrush phenomenon, being responsible for the large magnetizing currents due to the strong saturation produced by unsymmetrical magnetization. Both remanence and off-peak offsets are essentially stochastic phenomena from an applicational point of view. Remanence is rarely beyond 0.6 p.u. while the off-peak flux can only reach 1 p.u. under idealized infinite source conditions. The resultant d.c. offset will therefore be significantly less than 1.6 p.u. From the point of view of the computations it will appear as an arbitrary input which we do not chose to be too high in order to obtain inrush currents within the limits observed in tests.

Harmonic Domain Calculations

During the inrush phenomenon there are eddy currents in the laminations which render the flux distribution non-uniform. Therefore, a detailed analysis requires that the lamination be discretized into layers (or sublaminations, see Ref.[4]). By performing the calculations in this detailed way, we have found however that the non-uniformity of the flux distribution is insignificant at power frequency energization and the results are very closely the same as without spatial discretization. Because of this we have, as already mentioned, relegated the presentation of the analysis with sublaminations to the appendix. It may still be of significance for the examination of inrush phenomena at higher frequencies.

If the effect of eddy currents is ignored, no laminations and a fortiori no sublaminations are needed for the modeling. The basic equation, the equivalent in integral form of eqn.(A-1b) of the appendix, is

$$v = N\frac{d\Phi}{dt} \tag{2a}$$

or, in the harmonic domain,

$$V_h = Nj\omega h\Phi_h \tag{2b}$$

Equation (2b) can be used for all h except for $h=0$, because we do not have perfect d.c. variables, as $h=0$ would imply, but a slowly attenuating process. In the latter case, eqn.(2a) is used for the calculation of the time step Δt, as shown in the next section.

The Thevenin equivalent of the external circuit yields

$$V_h^T = V_h + Z_h^T I_h \tag{3}$$

The non-linearity of the iron core is given, similarly to eqn.(A-3), by

$$F = b_1\Phi + b_p\Phi^p + b_q\Phi^q \tag{4}$$

where F represents the magneto-motive force

$$F_h = NI_h \tag{5}$$

and

$$b_i = \frac{l}{A_{Fe}^i}a_i \tag{6}$$

Substitution of V_h from (2b) and of I_h from (5) into eqn.(3) yields

$$\frac{1}{N}Z_hF_h + j\omega hN\Phi_h = V_h^T \tag{7}$$

where Z_h represents the sum of the external and winding impedance. This equation has to be solved in conjunction with eqn.(4) whose linearized form in the harmonic domain [4] is of the form

$$\mathbf{J\Phi - F = C} \tag{8}$$

In equations (7) and (8) the unknowns are F_h and Φ_h for all h with the following exception. For $h=0$ eqn.(7) can not be used for the reasons explained earlier. Accordingly, we have one equation less and we eliminate therefore Φ_0 from the set of unknowns by specifying it as an input to the problem.

An efficient solution procedure of equations (7) and (8) is the following. From (7) we calculate F_h for $h\neq 0$, in terms of Φ_h for $h\neq 0$, and substitute it into (8). Thus the unknowns in (8) are Φ_h for $h\neq 0$ and F_0. After finding their values, we obtain all F_h for $h\neq 0$ (from (7)) and repeat the process for the converged solution.

The size of this problem depends on the number m of non-zero harmonics considered. Taking into account that the harmonics form complex conjugate pairs and adding the 0-order harmonic, the size of problem (8) results $2m+1$ in contrast with the much bigger size, $(2m+1)(n+1)$, in the case when the lamination is discretized into $2n$ sublaminations, as discussed in Appendix 1.

Calculation of Time Step

In our approach the time step Δt is variable and is calculated from the data already computed for two consecutive steady state images. We use equation (2a) for this purpose, written in terms of V_0 and Φ_0. The latter is known as a specified input, as discussed in the previous section. From the calculated F_0 we obtain I_0 from (5) and then V_0 from

$$V_0 = -R^T I_0 \tag{9}$$

which results directly from eqn.(3) with $V_h^T=0$.

Using the trapezoidal rule, eqn.(2a) will then yield

$$\Delta t = \frac{2N(\Phi_0^{(i+1)} - \Phi_0^{(i)})}{(V_0^{(i+1)} + V_0^{(i)})} \tag{10}$$

where the superscripts in parentheses indicate values taken before and after the step Δt.

General Algorithm

Figure 1 gives the chart of the two step algorithm used for the simulation of the inrush phenomenon. The block INRUSH performs the steady state calculation for each step i, while DELTAT calculates the time Δt between the states i and $i+1$.

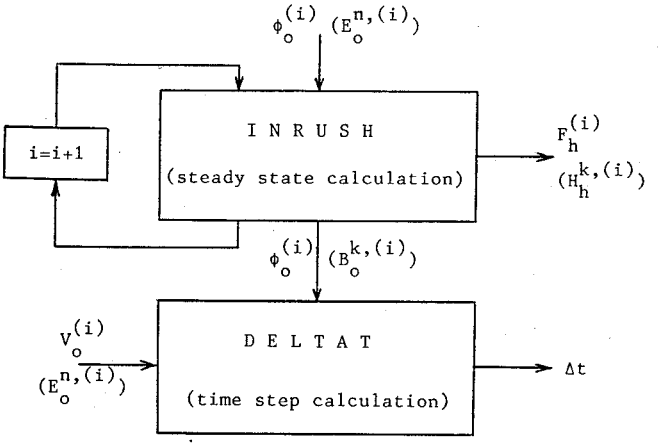

Fig.1 Block diagram of general algorithm. The variables in parentheses correspond to the modeling with sublaminations (Appendix 1).

The input information for INRUSH consists of the Thevenin impedance Z_h^T and voltage V_h^T, and the d.c. bias $\Phi_0^{(i)}$ chosen as a decreasing set of values with respect to i. This subroutine calculates all $\Phi_h^{(i)}$ and $F_h^{(i)}$. From these, $F_h^{(i)}$ is used for obtaining the inrush current, according to eqn.(5), while $\Phi_0^{(i)}$ is used in the second block.

Subroutine DELTAT performs the calculation of the time step of eqn.(10).

Three-Phase Transformer

We will not consider separately the single-phase energization of three-phase transformers because the phenomena are similar to those in single-phase transformers.

Even though the three-phase energization of a transformer is in general not simultaneous on the three phases, this does not affect the harmonic domain phenomena directly. Its effect is felt through the resultant magnitude of premagnetization flux on each limb of the transformer and it will be discussed in the next section.

D.C. Premagnetization

Remanence. We assume that the deenergization of the transformer is sequential and therefore a single-phase phenomenon for the last current to be interrupted. Consequently, there is a single limb with

maximal remanent flux. It returns almost entirely through the other limbs. The distribution of the return flux on the other limbs can be calculated based on their unsaturated reluctances. In the particular case of a five- legged core with a delta-connected winding, at the moment of deenergization the flux distribution on the three main legs has to closely satisfy the zero sum condition resulting from the induced voltages. Therefore, there will be no essential premagnetization of the side legs.

Off-Peak Switching. In the ideal case of simultaneous energization of the three phases, the resultant d.c. flux components have zero sum. This is still approximately true in the case of non-simultaneous switching in the case of a three-legged core and for any core construction in the case of delta winding connection. Therefore, the phenomenon is similar to that of remanence. The worst case appears when the maximal flux due to the two causes is on the same limb. Because of the voltage drop on the external impedance, the premagnetization due to off-peak switching will normally be well below its theoretical maximum and the resultant d.c. premagnetization will probably rarely exceed 1 p.u.

Harmonic Domain Calculations

As mentioned before, the flux distribution in the laminations is practically uniform. This permits to use the simplified approach without sublaminations, which is particularly important in the modeling of three-phase transformers.

Figure 2 represents the core construction of three and five-legged transformers. The nodes shown are at the confluence of three iron fluxes and, possibly, an air return flux. The associated graphs are shown in Fig.3 where the branches correspond to fluxes and single turns are shown to represent windings and the related m.m.f.'s for the meshes formed by closed flux paths. The frames represent the reference magnetic potential (on a perpendicular plane at the middle of the legs).

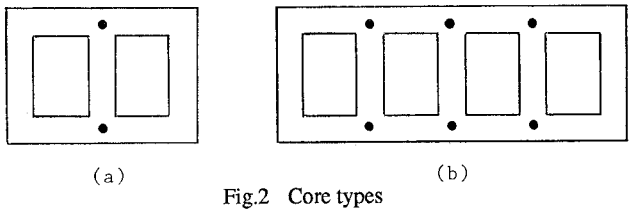

Fig.2 Core types

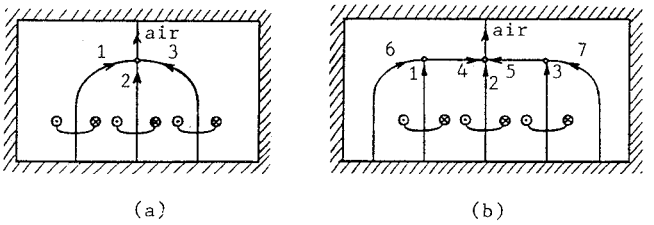

Fig.3 Graphs associated to the core types of Fig.2

Equations (2b) and (4), corresponding to the induced voltage and the nonlinear magnetization characteristic, are directly applicable for the three-phase case. We have to add also the nodal equations for the fluxes. For exemplification, we shall first refer to the three-legged core of Fig.2a. We have then

$$\Phi_h^1+\Phi_h^2+\Phi_h^3=\Phi_h^{air} \tag{11}$$

The magnetic mesh equations, for the example of Fig.2a and Fig.3a, are

$$F_h^1-F_h^2=I_h^aN-I_h^bN \tag{12a}$$

$$F_h^2-F_h^3=I_h^bN-I_h^cN \tag{12b}$$

$$F_h^3+F_h^{air}=I_h^cN \tag{12c}$$

In these equations each F_h at the left hand side represents an m.m.f. of a magnetic branch of a mesh, while the right hand side of the respective equation expresses the total mesh m.m.f. in terms of the ampere-turns of the loop. The superscript designates the limb or the winding, according to the context.

For the air return path we write

$$F_h^{air}=R_{magn}^{air}\Phi_h^{air} \tag{13}$$

where R_{magn}^{air} is the reluctance of the air return path. This has been assumed here to be linear and independent of frequency, but these restrictions could be easily relaxed. The value of R_{magn}^{air} can be estimated from design or from measurement data.

The above equations pertain to the three-legged core. Similar ones can be written for a five-legged core; see Appendix 2.

In order to express the interrelation between the windings and the external circuits, we have to consider the particular winding connections, see Fig.4.

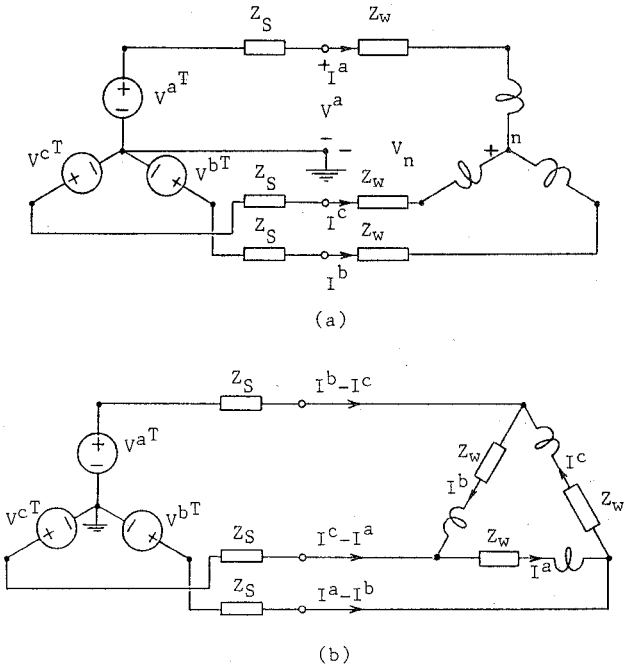

Fig.4 General supply layout for (a) Y and (b) Δ winding connections

In the case of a Y connection (Fig.4a), the relevant equations are, similarly to eqn.(7),

$$\frac{1}{N}Z_hF_h^a+j\omega hN\Phi_h^a=V_h^{a^T}-V_n \tag{14a}$$

$$\frac{1}{N}Z_hF_h^b+j\omega hN\Phi_h^b=V_h^{b^T}-V_n \tag{14b}$$

$$\frac{1}{N}Z_hF_h^c+j\omega hN\Phi_h^c=V_h^{c^T}-V_n \tag{14c}$$

The additional variable V_n, representing the neutral voltage, is directly specified as zero in the case of grounded neutral or remains as unknown, in the case of isolated neutral, in which case we add the constraint

$$I_h^a+I_h^b+I_h^c=0 \tag{15}$$

If the neutral is grounded through an impedance, eqn.(15) becomes

$$I_h^a+I_h^b+I_h^c=\frac{V_n}{Z_n} \tag{15a}$$

If the winding is Δ-connected (Fig.4b), the relevant equations are

$$Z_{w_h}I_h^a+Z_{s_h}(2I_h^a-I_h^b-I_h^c)+j\omega hN\Phi_h^a=V_h^{c^T}-V_h^{b^T} \tag{16a}$$

$$Z_{w_h}I_h^b+Z_{s_h}(2I_h^b-I_h^c-I_h^a)+j\omega hN\Phi_h^b=V_h^{a^T}-V_h^{c^T} \tag{16b}$$

$$Z_{w_h}I_h^c+Z_{s_h}(2I_h^c-I_h^a-I_h^b)+j\omega hN\Phi_h^c=V_h^{b^T}-V_h^{a^T} \tag{16c}$$

In these equations

$$I_h^a=F_h^a/N,\quad I_h^b=F_h^b/N,\quad I_h^c=F_h^c/N \tag{17}$$

In addition to the above equations, we have the fundamental nonlinear relation (4) between F and Φ. Since all the other equations (i.e. (11) - (15) or (11),(12),(13),(16) and (17) for the three-legged core) are linear, they are used to eliminate all other variables, so that the size of the resultant problem is determined by the number of nonlinear equation only. This number is related to the number m of non-zero harmonics considered and to the number n_m of independent magnetic meshes. For example, according to Fig.2a for a three-legged transformer, n_m=3, while from Fig.2b for a five-legged core, n_m=5. The total number of equations/unknowns is thus $(2m+1)n_m$. For m=15 harmonics, the problem size is then 93 for three legs and 155 for five legs.

POWER AND ENERGY BALANCE

It is known that the attenuation of inrush currents is due to losses but which losses are relevant is not a priori clear. It is clear however (see the section about the calculation of the time step) that the attenuation is essentially governed by the zero order harmonic. Since the latter does not directly produce losses in the iron, the attenuation will depend only on the external resistive losses due to the harmonic h=0. The computations we have performed have confirmed that the iron losses do not affect the rate of attenuation. As it will be shown later, this renders the detailed examination of the phenomena in the iron irrelevant to this study. Also, copper losses due to non-zero harmonics have no direct effect on attenuation.

Figure 5 serves to clarify the interrelation between losses and attenuation. It represents the power balance of supply and losses. The source power (A) (active and reactive) of fundamental frequency is first reduced by the losses (B) in the external circuit (including the winding) and the difference (C) enters the iron at its surface. The iron losses (D) are shown inside the lamination. They are produced by all non-zero harmonics. The remaining power (E) leaves the iron at its surface and corresponds to the Poynting vector for $h\neq1$. It covers the resistive losses in the external circuit, but only the component for h=0 is relevant to the attenuation.

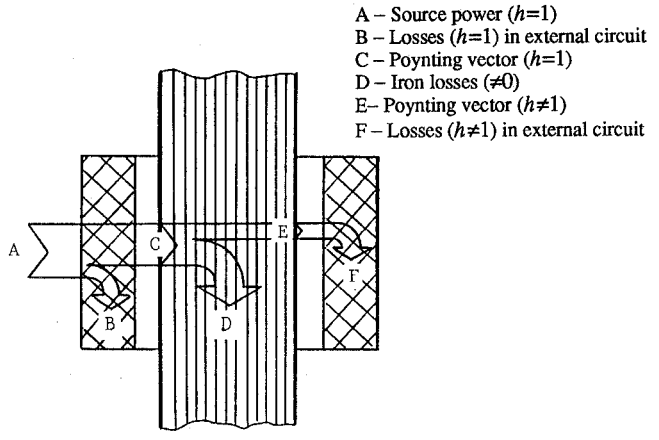

Fig.5 Active and reactive power balance diagram in external circuit and iron core

SIMULATION RESULTS

We consider as base case a 100/3 MVA/phase single or three-phase transformer energized from a 60 Hz, 115 kV, 60 km transmission line. The secondary is open circuited. The input impedance of the transformer is 0.6 + j1.1 Ω. The transmission line impedance is 6 + j24 Ω. The iron core of the transformer has laminations of $2d=0.3\times10^{-3}$ m thickness, with conductivity $\sigma=6\times10^{6}$ S/m. When discretized, we assume that they consist of $2n$=8 sublaminations. The harmonic domain calculations include harmonics up to order 15. The legs of the iron core have a height l=2 m and a cross-section area of A_{Fe}=0.385m^2. The number of turns is N=370. The base case level of d.c. premagnetization was assumed 0.4 T and B_{max}=1.65 T. The resulting inrush current is 0.91 kA (peak), by 28% bigger than the rated current.

Sublaminations

Sublaminations have been introduced (see references [4] and [5]) for the examination of internal phenomena in the laminations of the iron core. These are affected by the distribution of eddy currents which determine a major part of the iron losses. The inrush phenomenon is, on the other hand, governed by the circuit external to the iron core. The detailed representation of the laminations is therefore not needed for the computation of inrush currents. This fact has been confirmed by numerous tests of transformer energization with and without the use of sublaminations in the iron core modeling. For any external impedance and for any level of premagnetization, the results were the same, with usually much less than 0.25% error (the latter at energization from an infinite bus). While the flux and eddy current distribution in the sublaminations is of no consequence, and only the variables at the surface of the lamination are of significance in the calculation of inrush currents, it is interesting to note that the uniform flux distribution (around peak values) inside the lamination, due to saturation, observed (see [4] and [5]) in the case of symmetrical magnetization, is not modified by the asymmetry of the magnetization characteristic for the inrush phenomenon; see Fig.6a. The individual harmonics, in particular the d.c. component are, however, non-uniformly distributed about the cross-section. Fig.6b represents the space-time variation of the corresponding magnetic field intensity.

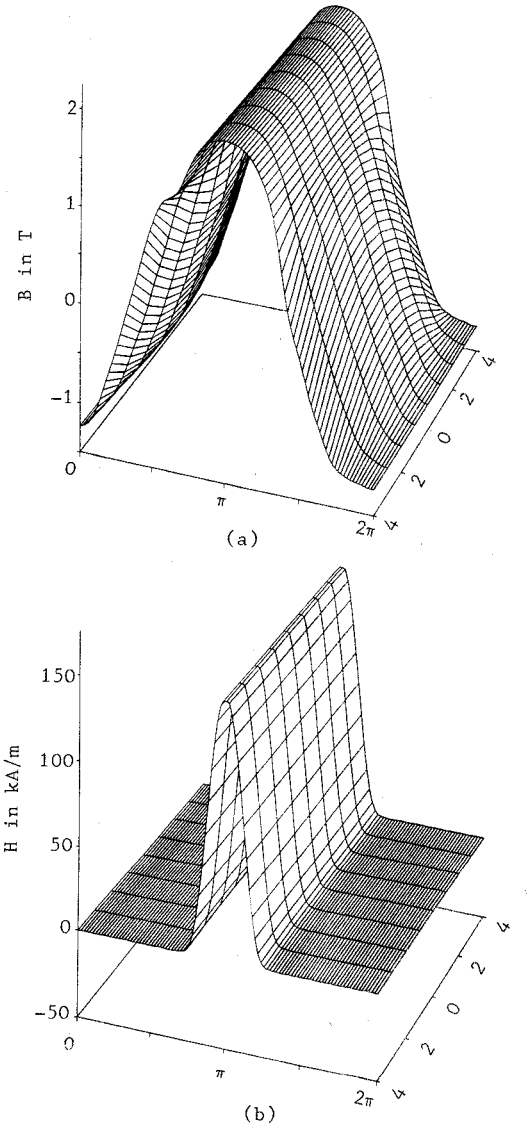

Fig.6 Variation of (a) B and (b) H in time and space during inrush with 0.4 T d.c. offset (base case)

Effect of External Circuit Parameters

The factors which have a potentially important effect on the inrush phenomenon are:

- $Z^T=R^T+jX^T$, the Thevenin impedance of the external circuit as seen from the surface of the iron core (i.e. with the winding impedance included)
- V^T, the Thevenin source voltage.

The Thevenin resistance R^T plays a major role in the attenuation of the inrush current. This can be locally characterized by a time-varying time-"constant", equal to the ratio $(L_{dyn}+L^T)/R^T$. Fig.7 illustrates the attenuation effect in terms of I_{max}, the peak value of the inrush current. The common parameters for the two curves are: V^T, B_0=0.4 T and L^T. As expected, the curve with bigger R^T has proportionally larger attenuation. The common starting point of the two curves corresponds to the fact that the other parameters are the same. These curves have been obtained using subroutine DELTAT shown in Fig.1 with ten calculated points.

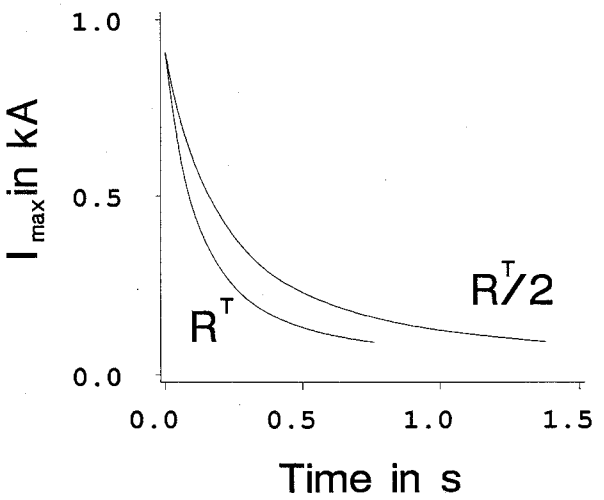

Fig.7 Inrush current attenuation curves for different external resistances

The magnitude of the reactance X^T would have little direct effect on the magnitude of the inrush current as it is normally small compared to the reactance of the iron core, even when the latter is saturated. However, it affects the point of operation on the magnetization characteristic so that with larger L^T the inrush current will decrease. For instance, compared to the base case, doubling of L^T reduces the inrush current by 32%. The largest inrush current will of course result in the case of energization from an infinite bus: about 3 times the base value.

The Thevenin source voltage V^T affects both the magnitude and the attenuation of the inrush current. The computed results have shown that, as expected, the magnitude of the inrush current increased and decreased in the same way as the voltage. A 5% increase in voltage produced a 42% increase in the magnitude of the inrush current for the base case. The time to one tenth of the initial current, $t_{1/10}$ varies in inverse relation to the magnitude of the voltage. For instance, for the rated voltage we have $t_{1/10}$=0.76 s, while for a voltage smaller by 5% $t_{1/10}$=0.99 s. The reason is that at lower voltage levels, i.e. less saturation, L_{dyn} is larger.

We note that the attenuation of the inrush current is faster than that of B_0 and other related d.c. components, due to the strong saturation effects produced by higher values of B_0.

Effect of Premagnetization Level

Fig.8 gives the relation of the initial inrush current (RMS value and magnitude) and the d.c. premagnetization. An 8-fold increase of the d.c. premagnetization (from 0.1 to 0.8 T) results in a 30-fold increase of the inrush current. By performing the steady state calculations at decreasing premagnetization levels and calculating the related time intervals, we obtain the time variation of the inrush current as shown in Fig.9, which serves to illustrate the basic idea of this paper.

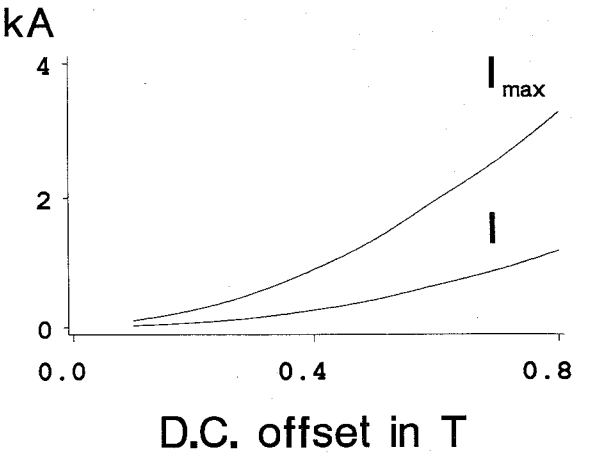

Fig.8 Dependence of the initial inrush current (RMS value I and magnitude I_{max}) on the d.c. premagnetization

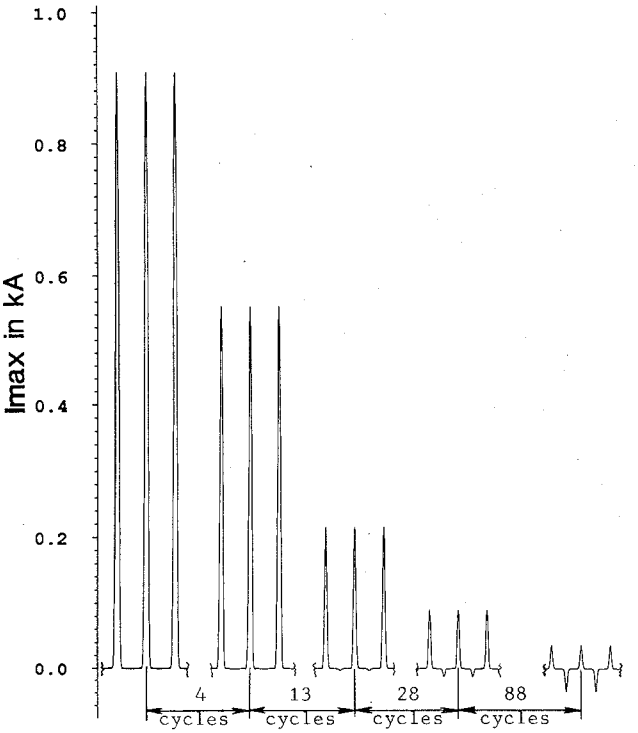

Fig.9 Attenuation process of inrush current represented by consecutive steady state images

Three-Phase Energization

Our general remark on the three-phase inrush phenomenon is that the magnitude of the currents are, for all other problem parameters equal, smaller in the three-phase case than in single-phase transformers. This could be explained by the fact that the reluctance of the magnetizing path is smaller in the case of three-phase transformers. For the three-legged core with maximal premagnetization on the middle leg (which gives the largest currents) of 0.4 T, we have obtained, in the case of Y connection with the neutral directly connected to the source, the following peak values: i_a=0.48 kA, i_b=0.87 kA, and i_c=0.48 kA (see Fig.10). For a single-phase transformer the initial inrush current, for the base case conditions, was 0.91 kA. Consequently, the calculation of inrush currents using a single-phase approach gives conservative values. Therefore, for more realistic and accurate results the computations have to be performed for the actual three-phase transformer unit.

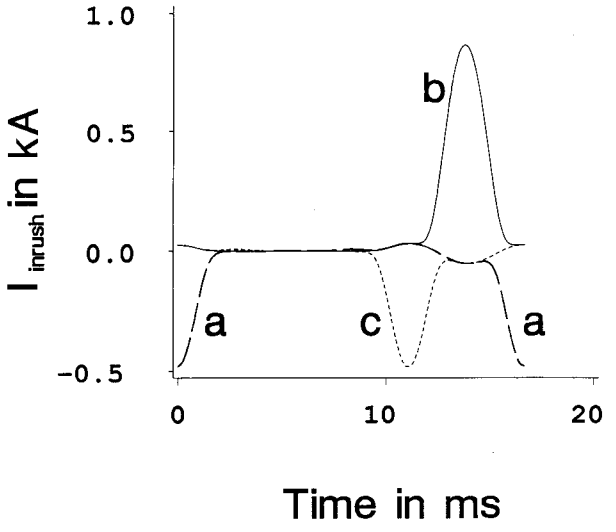

Fig.10 Inrush currents in three-phase transformer

We note that the results are strongly affected by the winding connection and also by the presence of additional legs for flux return (five-legged core). If the neutral is not directly connected to the source, the inrush currents result smaller, due to the suppression of zero sequence components in the fundamental and harmonics. For a five-legged core derived from the three-legged core of the previous paragraph, the peak inrush currents for the base case are i_a=0.18 kA, i_b=0.89 kA, and i_c=0.18 kA, due to the different distribution of the d.c. premagnetization flux.

CONCLUSIONS

The paper has presented a novel approach for the investigation of the inrush phenomenon in single and three-phase transformers. It consists in the calculation of a sequence of quasi steady state images using harmonic domain computation. Thus lengthy time domain simulations with the related round-off and truncation errors are avoided.

An important result of the analysis is the fact that the attenuation of inrush currents is not affected by the eddy current and hysteresis losses in the iron. Therefore no discretization of the laminations is needed, which considerably simplifies the computations without any loss of accuracy. The attenuation is solely determined by the resistance of the external circuit and the total inductance of the circuit, including also that of the iron core.

The paper shows how remanence and off-peak switching combine to establish the initial bias which determines the magnitude of the inrush current.

It is of practical importance that the calculation of inrush currents in three-phase transformers, of any type of construction and winding connection, is computationally feasible. It is, however, not always needed because the single-phase calculation gives conservative results.

ACKNOWLEDGEMENTS

Financial support from the Natural Sciences and Engineering Research Council of Canada is gratefully acknowledged. The first author wishes to express his appreciation to the Faculty of Electrical Enginnering of the University of Belgrade for his study leave at the University of Toronto.

REFERENCES

[1] A. Greenwood, "Electrical Transients in Power Systems", Wiley - Interscience, 1971.

[2] D. Povh and W. Schultz, "Analysis of Overvoltages Caused by Transformer Magnetizing Inrush Current", IEEE Trans. on Power Apparatus and Systems, Vol. PAS-97, No.4, July/August 1978, pp. 1355-65.

[3] "Electrical Engineering Handbook", Siemens AG, Heyden & Son Limited, 1976.

[4] A. Semlyen and N. Rajaković, "Harmonic Domain Modeling of Laminated Iron Core", IEEE Paper No. 88 WM 047-3.

[5] N. Rajaković and A. Semlyen, "Harmonic-Domain Analysis of Field Variables Related to Eddy Current and Hysteresis Losses in Saturated Laminations", IEEE Paper No. 88 SM 548-0.

APPENDICES

1. Steady State Solution with Sublaminations for Specified E_0

For the phenomena inside the laminations we use Maxwell's equations

$$\frac{\partial H}{\partial x} = \sigma E \tag{A-1a}$$

$$\frac{\partial E}{\partial x} = \dot{B} \tag{A-1b}$$

or equivalently, their combination

$$\frac{\partial^2 H}{\partial x^2} = \sigma \dot{B} \tag{A-2}$$

We add to these the nonlinear relation between H and B, used in reference [4]

$$H = a_1 B + a_p B^p + a_q B^q \tag{A-3}$$

As in reference [5], hysteresis is modeled by using a complex value for a_1 in the harmonic domain calculations.

We discretize the lamination of thickness $2d$ into $2n$ sublaminations of thickness Δx. Sublamination or layer k is between discretization points $k-1$ and k, $k=0$ being in the middle and $k=n$ at the surface of the lamination. The field variables will have the discretization points k indicated as superscripts and the harmonic order h by a subscript. If m is the number of harmonics considered, then the total number of variables related to one field quantity (for instance B) is $m(n+1)$.

Transition into harmonic domain and discretization into sublaminations yields [4],

$$H_h^{k+1} - 2H_h^k + H_h^{k-1} = c\frac{\dot{B}_h^{k+1} + 10\dot{B}_h^k + \dot{B}_h^{k-1}}{12} \tag{A-4a}$$

$$4(H_h^n - H_h^{n-1}) + c(\dot{B}_h^n + \dot{B}_h^{n-1}) - 4c_o E_h^n = 0 \tag{A-4b}$$

where

$$c = \sigma(\Delta x)^2 \quad \text{and} \quad c_o = \sigma(\Delta x)$$

Eqn.(A-4a) is used for $k=0...n-1$ while eqn.(A-4b) has been written for $k=n$ and provides the interface for the Thevenin equivalent of the external circuit, which includes the impedance of the winding,

$$E_h^T = E_h^n + Z_h'^T H_h^n \tag{A-5}$$

where the field related quantities E_h^n, H_h^n and E_h^T, $Z_h'^T$ can be expressed in terms of circuit quantities and design data, as follows:

$$E_h^n = \frac{d}{NA_{Fe}} V_h \tag{A-6a}$$

$$H_h^n = \frac{N}{l} I_h \tag{A-6b}$$

$$E_h^T = \frac{d}{NA_{Fe}} V_h^T \tag{A-6c}$$

$$Z_h'^T = \frac{ld}{N^2 A_{Fe}} Z_h^T \tag{A-6d}$$

Here A_{Fe} and l are the cross-section area and the length of the iron core, N the number of turns of the winding, and V_h, I_h and V_h^T, Z_h^T are variables of the Thevenin equivalent of the external circuit, as seen from the surface of the lamination packet. In eqn.(A-5) the Thevenin voltage source E_h^T has a given non-zero value for the first harmonic and is (normally) zero for all other harmonics. This equation permits to eliminate the variables E_h^n from eqns.(A-4) and a harmonic domain version of eqn.(A-3) serves to replace all H_h^k. We have thus only B_h^k as unknowns in the final set of equations. One important remark is however in place here:

for h=0 eqns.(A-1b) and (A-2) can not be used because we do not in fact have perfect d.c. variables, as h=0 would imply, as mentioned in the main text. Therefore these equations will only be used later for the calculation of Δt, as shown in the main text. By analogy to the procedure there, one may wish to specify all B_0^k. However, we do not know their distribution over the sublaminations, and computations have shown that it is non-uniform. Consequently, a good estimate for B_0^k can not be made and the following approach has been taken to solve this problem.

The unusable equations had to be replaced by an equal number (n+1) of valid equations. These are obtained as the discretized form of (A-1a) (with E_h^k specified) in conjunction with eqn.(A-3), and the equation which specifies the value E_0^n of the field intensity corresponding to h=0 at the surface of the lamination. Thus E_0^k, for k=0,1,...n, is an input to our problem and has to be chosen in a way to produce some predefined value of premagnetization. This assumes that the space distribution of E_0^k is known.

Concerning the problem of the space distribution of E_0^k, we note that H is related to E by integration (see eqn.(A-1a)) and therefore is almost perfectly constant, irrespective of the distribution of E_0, since the actual values of E_0 are very small. Therefore, it was found reasonable to assume a linear distribution pattern for E_0 which corresponds to a perfectly uniform attenuation process in all layers, according to eqn.(A-1b).

The resultant set of nonlinear equations, **f(B)=0**, is solved by Newton's method

$$\mathbf{J}\,\Delta\mathbf{B} = -\mathbf{f} \tag{A-7}$$

boldface being used for harmonic vectors and the related Jacobian matrix.

The time step Δt is calculated from the data already computed for two consecutive steady state images. Recall that the input for the latter was E_0^n, the value of E_0 at the surface of the lamination, which has also defined the other values E_h^k because of the assumed linear distribution. The result of the calculation gave all B_0^k (among other variables), so that the average value B_0^{ave} is readily available. Then, by integrating eqn.(A-1b) over a half lamination, we obtain

$$E_0^n = \dot{B}_0^{ave} d \tag{A-8}$$

Using the trapezoidal rule, eqn.(A-8) yields

$$\Delta t = \frac{2(B_0^{ave,(i+1)} - B_0^{ave,(i)})d}{(E_0^{n,(i+1)} + E_0^{n,(i)})} \tag{A-9}$$

where the superscripts in parentheses indicate values taken before and after the step Δt.

Figure 1 gives the chart of the two step algorithm used for the simulation.

2. Magnetic Circuit Equations for Five-Legged Core

According to Fig.2b, the magnetic nodal equations are

$$\Phi_h^1 - \Phi_h^4 + \Phi_h^6 = 0 \tag{A-10a}$$

$$\Phi_h^2 + \Phi_h^4 + \Phi_h^5 = \Phi_h^{air} \tag{A-10b}$$

$$\Phi_h^3 - \Phi_h^5 + \Phi_h^7 = 0 \tag{A-10c}$$

In these equations a return flux through air is shown only for the middle leg of the transformer, since branches 6 and 7 effectively shunt out the respective air return paths.

The independent magnetic mesh equations are

$$F_h^1 - F_h^6 = NI_h^a \tag{A-11a}$$

$$F_h^1 - F_h^2 + F_h^4 = NI_h^a - NI_h^b \tag{A-11b}$$

$$F_h^2 - F_h^3 - F_h^5 = NI_h^b - NI_h^c \tag{A-11c}$$

$$F_h^3 - F_h^7 = NI_h^c \tag{A-11d}$$

$$F_h^5 + F_h^7 + F_h^{air} = 0 \tag{A-11e}$$

Nikola Rajaković was born in Yugoslavia in 1952. He graduated from the University of Belgrade where he also received his M.Sc. and Ph.D. degrees. He is now an assistant professor in Power Systems at the same university. He has published over twenty papers and one textbook, and has worked in numerous power system projects. His present research interest is in Harmonic Modeling and Optimization of Power Systems.

Adam Semlyen was born and educated in Rumania where he obtained a Dipl. Ing. degree and his Ph.D. He started his career with an electric power utility and held academic positions at the Polytechnic Institute of Timisoara, Rumania. In 1969 he joined the University of Toronto where he is a professor in the Department of Electrical Engineering. His research interests include the Steady State and Dynamic Analysis of Power Systems, Electromagnetic Transients, and Power System Optimization.